

## HIGHER ORDER MODE WAKEFIELD SIMULATIONS AND BEAM DYNAMICS SIMULATIONS IN THE ILC MAIN LINACS

R.M. Jones, and C. Glasman, Cockcroft Institute of Science and Technology, Daresbury, Cheshire WA4 4AD, UK, and University of Manchester, Manchester M13 9PL, UK

### Abstract

The progress of 2820 electron (and positron) bunches down the main linacs of the ILC (International Linear Collider) can readily give rise to dipole modes which disrupt the progress of the beam. We investigate the transverse modes which are excited and monitor the resulting emittance dilution which occurs down the linac. At present there are two design configurations for the ILC: the BCD (Baseline Configuration Document) [1] and the ACD (Alternate Configuration Document). We investigate the wake fields and beam dynamics for an ACD known as the re-entrant cavity.

### INTRODUCTION

The main linacs of the ILC will consist of more than 17,000 cavities which accelerate the electron (positron) beam from 5 GeV up to a center of mass energy of 500 GeV and in a proposed upgrade to 1 TeV. The present BCD relies on TESLA-style cavities and aims for an accelerating gradient of 35 MV/m. In order to reduce the number of accelerating cavities there is significant research being conducted into methods of increasing the gradient to 50 MV/m or more. Increasing the accelerating gradient in TESLA-style cavities leads to a concurrent increase in the maximum magnetic field on the walls of the cavity and this results in the superconductivity of the cavity breaking down [2]. Reshaping the cells of the cavities allows the ratio of the peak magnetic field to the accelerating gradient to be reduced compared to that of the TESLA shape. There are two main ACD designs which aim at reducing the field in this manner



Figure 1: Single-cell from TESLA cavity (left) and a corresponding cell from a re-entrant cavity (right) fabricated by the Cornell University SRF group [6].

and these are known as: LL (Low Loss) [3], and RE (Re-Entrant) [4] cavities. The former cavity also exists in a variant known as the ‘Ichiro’ cavity [5]. However in this paper, we focus on the latter design, the RE cavity. The main difference in the RE design compared to TESLA is

in the removal of the straight connecting section between the iris and cavity regions –both ellipses are directly contacting. For the purpose of comparison, the RE and TESLA single-cells are illustrated in Fig 1 [6]. There have been several optimized designs but in this paper we focus on a design which reduces the ratio of the peak magnetic field to the accelerating field by 10 % compared to that of the TESLA cell ( $H_{pk}/E_{acc} = 37.8 \text{ Oe/MV}$  [7]) but with a 20% increase in the peak electric field ( $E_{pk}/E_{acc} = 2.40$ ). However, the enhanced field emission that occurs with the increase in the peak surface electric field is not thought to be a cause for concern as surface treatment techniques such as high pressure rinsing have been shown to cope with surface gradients as high as 70-80MV/m with little field emission. Furthermore, there is no fundamental limit to the surface electric field up to 100 - 200 MV/m [2]. This design maintains the same iris radius as the TESLA design, viz., 35 mm. Thus, the short-range wake, will not change appreciably, and the cavity-to-cavity alignment tolerances will also be largely unchanged.

Nonetheless, the new design will repartition HOMs (Higher Order Modes) excited by the transit of the beam through the cavities and thus the long-range wake field will differ from that in the TESLA cavities. This may well change the beam dynamics and in the worst case give rise to trapped modes which can seriously disrupt the luminosity of the colliding beams. In accelerating the trains of electron (and counter-propagating electrons) it is important to maximise the luminosity of the colliding beams at the interaction point. The luminosity is given by:  $L = f n_1 n_2 (4\pi\sigma_x\sigma_y)^{-1}$ , where  $f$  is the collision

frequency,  $n_1$  and  $n_2$  are the number of particles in each of the colliding bunches and the beam dimension in the horizontal (vertical) plane is given by:  $\sigma_{x(y)} = (\beta_{x(y)}\epsilon_{x(y)})^{1/2}$ . Here,  $\epsilon_{x(y)}$  is the horizontal (vertical) emittance and  $\beta_{x(y)}$  is the horizontal (vertical) focusing function. Thus, in order to maximize  $L$  it is required to minimize the emittance. For this reason it is important to avoid any emittance dilution that may occur due to HOMs (Higher Order Modes) being excited in the cavities. These HOMs give rise to a wakefield, excited by each bunch in the train of 2820 bunches. Trailing bunches feel the effect of the wakefield in two important ways: firstly, an energy spread is induced on them and secondly, they are kicked transverse to longitudinal axis of the cavity. The latter effect can readily give rise to a growth in the emittance of the beam.

In this paper we investigate the HOMs through detailed simulations of the characteristic eigen-modes of the

cavities and in a beam dynamics study in which we track the beam through the complete linac. The detailed geometrical parameters used in this study are given in [7].

This paper is organized such that the next section discusses detailed simulations of the Brillouin diagrams associated with infinitely periodic single-cell systems and the eigen-modes of the 9-cell cavities. This subsequently leads to a calculation of the HOM wakefields. The penultimate main section completes the analysis, with a beam dynamics study in which the emittance dilution due the transverse long-range wakefields is monitored down the linac

## TRANSVERSE WAKEFIELDS

### *Eigenmodes of Cavity*

The energetic electron beam excites a series of HOMs by traversing each of the accelerating cavities. Each cavity is composed of 9 cells. The modes excited by the beam may be decomposed into a series of eigenmodes, each of which is confined to a series of characteristic pass-bands. This band structure is illustrated in the form of a Brillouin diagram in Fig. 2. We obtained the continuous curves of this periodic structure using the finite difference computer code GdfidL [8]. A typical mesh used in these eigenvalue calculations is displayed in Fig 3. The characteristic eigen-frequencies of each band are calculated for a specified phase advance. The point at which the free-space dispersion curve, or light line, intersects each of the

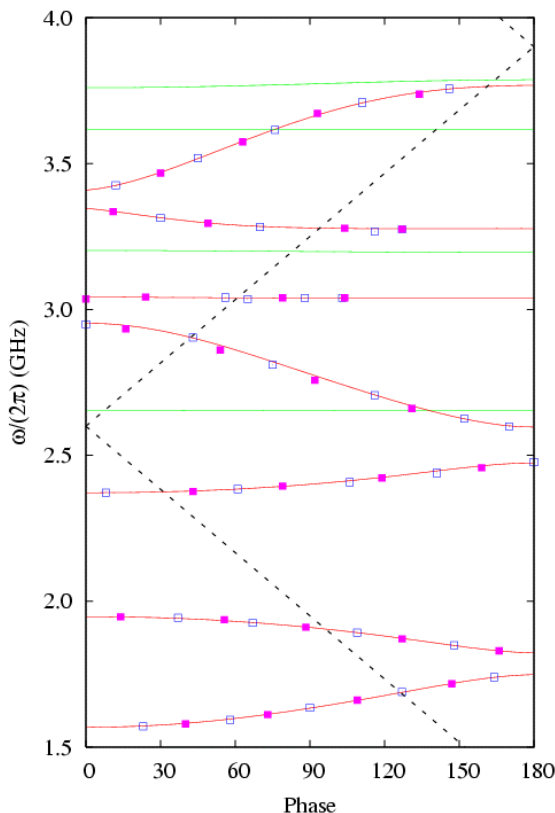


Figure 2: Brillouin diagram for 7 dipole bands. The light line is shown dashed.

curves corresponds to the synchronous point. Maximum interaction with the beam occurs at these intersection points. Each bunch excites these modes as it traverses the



Figure 3: GdfidL mesh consisting of  $1.45 \times 10^6$  elements for a one quarter section of a single RE cell. Each mesh element is separated from its neighbour by 1mm.

accelerating cavities and successive bunches will experience the maximum influence of this e.m. field at or close to the synchronous point.

The modes excited by the beam are calculated by considering a full 9-cell cavity with appropriate symmetry conditions. We utilise a symmetry plane, which splits the cavity into 4.5 cells and by making separate simulations with magnetic and electric walls at the symmetry planes we are able to recover the modes of the complete cavity. The phase advance per cell,  $\phi$ , is calculated for each of the discrete eigen-frequencies using:

$$\cos \phi(z) = \frac{E_z(r, z + L_{\text{cell}}) + E_z(r, z - L_{\text{cell}})}{2E_z(r, z)} \quad (1)$$

where for the infinitely periodic structure modeled, we have made use of the Floquet condition:

$$E_z(r, z) = \exp(-i\phi) E_z(r, z + L_{\text{cell}}). \quad (2)$$

The e.m. field that corresponds to these eigenmodes will impart a transverse force to the beam. This e.m field is conveniently represented as a wakefield [9], which will kick the beam transversely to the direction of acceleration. We decompose this wakefield into a series of kick factors [9] and eigen-frequencies. These kick factors are analysed in the next sub-section.

Finally, we note that modes localized, or trapped, in the central cells of the cavity are particularly disruptive to the beam. A typical trapped mode is illustrated in Fig. 4.

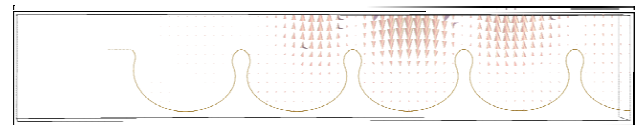


Figure 4: Trapped mode in RE cavity at 3.0396 GHz.

### *Multi-Cell Analysis of Kick Factors*

The modes which impart a transverse kick to the beam, corresponding to the points in Fig. 2, are analysed in terms of characteristic kick factors. Armed with the knowledge of these parameters allows the wakefield to be determined and the beam dynamics studied issues related to tracking the beam down the complete linac to be studied. We have calculated the kick factors of 7 bands. However, in order to reduce the computational time in

beam dynamics simulations we have limited the modes to 12 of the largest. These modes are presented in Table 1.

Table 1: HOM Parameters of 9-cell RE Cavity.

$\omega/2\pi$ (GHz)	$K_n$ (V/pC/mm/m)
1.6611	0.003890
1.6892	0.005228
1.7169	0.004274
1.8303	0.003178
1.8711	0.012398
1.8926	0.008581
1.9113	0.009179
1.9259	0.007135
2.3721	0.013896
2.3764	0.013941
2.3845	0.007277
2.3946	0.003904

### Transverse Wakefield

The long-range transverse wakefield, at a distance  $s$  behind the first bunch, is calculated from the modal sum:

$$W(s) = 2 \operatorname{Im} \left\{ \sum_{n=1}^N K_n e^{i\omega_n s/c} e^{-\omega_n s/2Q_n c} \right\} U(s) \quad (3)$$

where  $N$  is the number of modes,  $U(t)$  is the unit step function, the  $n^{\text{th}}$  mode has a quality factor of  $Q_n$ , a kick factor  $K_n$  and a synchronous frequency  $\omega_n/2\pi$ . Over the length of the bunch train, the wakefield varies rapidly and it is convenient to display the envelope of the wakefield and this is obtained from the absolute value of the modal sum (effected by taking the absolute, rather than the imaginary part of the sum in Eq. (3)). The envelope of the transverse wakefield is illustrated in Fig. 5 for the parameters given in Table 1. We utilize this wakefield in

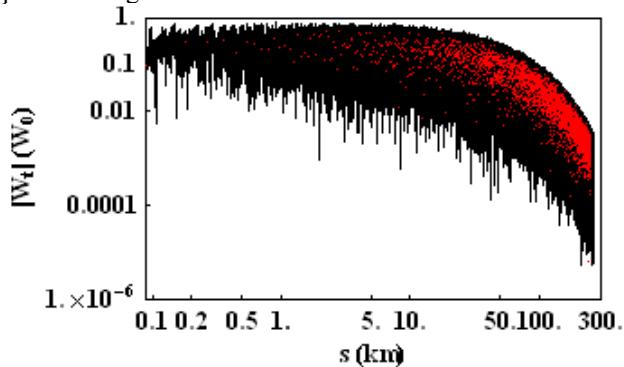


Figure 5: Transverse wakefield for 9-cell RE cavity ( $W_0=0.19$  V/pC/mm/m and,  $Q = 10^6$  for all modes).

beam dynamics studies in which we track the beam down the entire linac, using the code LIAR[10], whilst monitoring the emittance dilution.

### BEAM DYNAMICS

At the nominal bunch spacing, the emittance dilution that results due to the long-range wakefields amounts to approximately 38 % of the injected emittance (see Fig. 6).

However, a remarkably small change in the bunch spacing ( $\sim 0.0085$  %), or a corresponding change in all frequencies, results in more than 400 % dilution in the emittance. This is in contradistinction to the TESLA cavities, which showed little sensitivity to small systematic frequency errors [11]. The modes associated with these peaks in emittance dilution are already under study with a view to ascertaining the  $Q_s$  necessary to reduce overall levels of the emittance dilution.

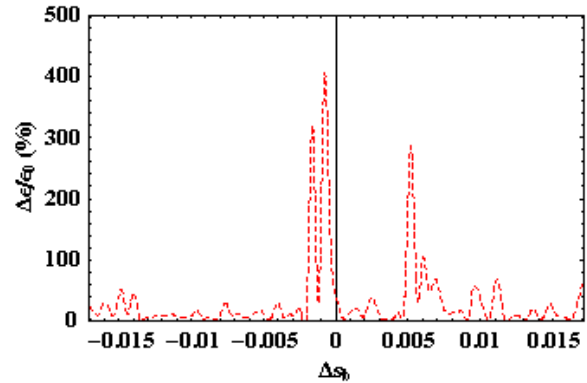


Figure 6: Emittance dilution along linac for a  $\sigma_y$  beam offset versus  $\Delta s_b$ , percentage change in the bunch spacing.

### CONCLUSIONS

Additional studies on the RE cavities are needed; in particular a systematic study of the damping  $Q_s$  is already in underway. Furthermore, care must be taken to ensure modes trapped at 2.6539 GHz, 3.0396 GHz and 3.0425 GHz are properly damped.

Reducing the radius of the irises of the cavities is another means to enable high gradients to be obtained. Further studies will be made on the wakefields and alignments imposed in RE cavities with a reduced iris.

### ACKNOWLEDGEMENTS

We are pleased to acknowledge the unfailing support and timely advice of W. Bruns, the author of the code GdfidL. We acknowledge the encouragement of H. Padamsee in this work and are grateful to V. Shemelin for supplying the necessary geometrical parameters.

### REFERENCES

- [1] Baseline Configuration Document, December, 2005. [http://www.linearcollider.org/wiki/doku.php?id=bcd:bed\\_home#latest\\_official\\_version\\_of\\_bcd](http://www.linearcollider.org/wiki/doku.php?id=bcd:bed_home#latest_official_version_of_bcd).
- [2] R.L. Geng, 2005, Invited talk at 12<sup>th</sup> International Workshop on RF Superconductivity, July 10-15, NY.
- [3] J. Sekutowicz, 2004, Presented at first ILC Workshop, November 13-15, KEK, Japan.
- [4] R.L. Geng *et al.*, 2005, Presented at 2005 Particle Accelerator Conference, Knoxville, TN.
- [5] K. Saito *et al.*, 2005, Presented at 12<sup>th</sup> International Workshop on RF Superconductivity, July 10-15, NY.
- [6] <http://www.lns.cornell.edu/Research/AP/SRF/WeHome.html>.
- [7] V. Shemelin and H. Padamsee, 2005, SRF050808-06.
- [8] <http://www.gdfid.de/>.
- [9] P.B. Wilson, 1989, SLAC-PUB-4547.
- [10] R. Assman *et al.*, LIAR, 1997, SLAC-PUB AP-103.
- [11] R.M. Jones and N. Baboi, 2005, SLAC-PUB-11235